Chemical Papers (2024) 78:3959–3969
https://doi.org/10.1007/s11696-024-03366-w

ORIGINAL PAPER

Bacterial cellulose from mother of vinegar loaded with silver nanoparticles as an effective antiseptic for wound-healing: antibacterial activity against *Staphylococcus aureus* and *Escherichia coli*

Ana B. Morales-Cepeda[1] · Abigail M. Díaz-Guerrero[1] · Antonio S. Ledezma-Pérez[2] · Carmen N. Alvarado-Canché[2] · José L. Rivera-Armenta[1]

Received: 13 June 2023 / Accepted: 10 February 2024 / Published online: 4 March 2024

Abstract

Bacterial cellulose (BC) has gained attention in recent years due to its high purity and multiple applications in the biomedical and pharmaceutical fields, and mothers of vinegar are a promising source of low-cost BC that can be easily obtained from any variety of vinegar. Silver nanoparticles (AgNPs) are known for their antimicrobial activity as well as their use as antiseptics on healing wounds. For this research, BC-AgNPs films were synthesized, and their antibacterial activity against *Staphylococcus aureus* and *Escherichia coli* was evaluated. The BC films were obtained from mothers of vinegar from two varieties (apple vinegar and cranberry vinegar) and were used as support for AgNPs at 5, 25, 41, 69, 116 and 324 ppm. All the films added with AgNPs achieved growth inhibition of 99–100% for both bacterial species, exhibiting values of antibacterial effectiveness (*R*) between 3.37 and 7.72. The BC-AgNPs films presented a slightly higher antibacterial activity against *S. aureus*, but the difference was negligible, and the composites were effective to inhibit the growth of both bacteria. The results show that the BC-AgNPs films synthesized from mothers of vinegar have potential for wound-healing purposes and that they are effective with silver concentrations as low as 5 ppm.

Graphical Abstract

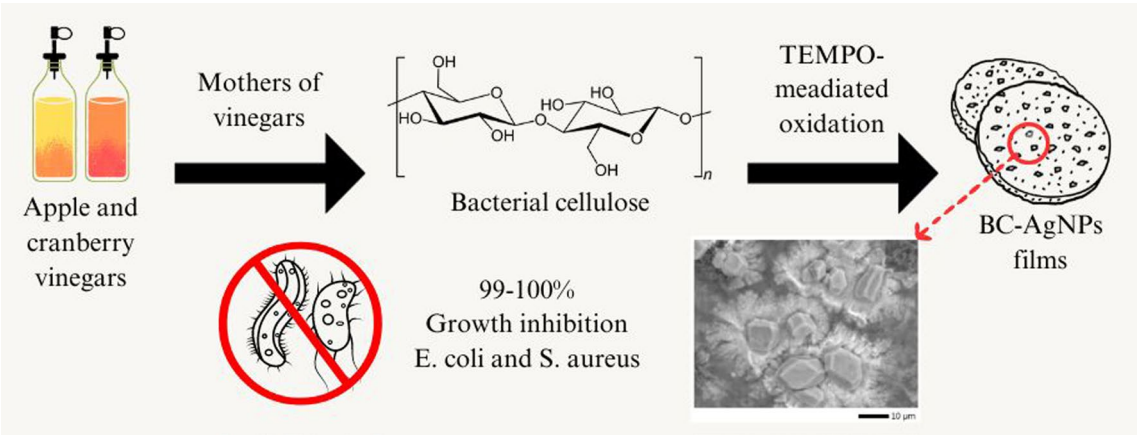

Keywords Silver nanoparticles · Bacterial cellulose · Antibacterial activity · Antimicrobial activity · Mother of vinegar

Extended author information available on the last page of the article

Introduction

Cellulose and its derivatives have gained the attention of the scientific community in recent years due to its easy fabrication, biodegradability, biocompatibility and multiple applications in the biomedical and pharmaceutical fields, including its capacity to adsorb, immobilize and enhance the surface area of nanoparticles with antimicrobial properties, acting as a drug delivery system (Das et al. 2022; Ciolacu et al. 2020; Norrrahim et al. 2021).

Most cellulose is extracted from plants such as cotton, flax, hemp, jute or bamboo, as well as from a wide variety of trees (Bakri et al. 2022), and it can be obtained either in the form of nanofibers (CNF) or nanocrystals (CNC). However, obtaining cellulose from plants has several disadvantages. Cellulose extracted from plants is combined with other natural polymers found in plants, such as lignin, pectin and hemicellulose (Wang et al. 2019), and it results necessary to purify it before its use. This purification requires a combination of mechanical methods such as grinding, crushing, filtering or sieving with chemical separation methods assisted by acidic or basic solvents, or biological methods assisted by enzymes (Radotić and Mićić 2016). Then, after the separation process, the pure cellulose must either undergo a mechanical shearing to produce nanofibers with diameters of less than 100 nm or through a strong acid hydrolysis to soften and break down the less crystalline regions in the material and produce nanocrystals (Salama et al. 2021). Added to the energy and resources that are necessary to obtain CNF or CNC from plants, as well as to the pollution produced by the chemical waste, another problem to consider is that the sizes of the obtained particles can vary in a wide range, resulting in low reproducibility for experiments involving these materials (Lukova et al. 2023).

Obtaining bacterial cellulose (BC), on the other hand, is a simpler and environmentally friendly process. Bacterial cellulose can be synthesized by bacteria of the genera *Acetobacter*, *Agrobacterium*, *Azotobacter*, *Rhizobium*, *Sarcina*, *Alcaligenes* or *Pseudomonas* using a wide variety of precursors, including hexanoates, hexoses, dihydroxyacetone, pyruvate and glycerol (Lahiri et al. 2021). The resulting material is a high-purity polymer that does not contain the hemicellulose, pectin and lignin of the cellulose obtained from plants, which makes of its purification a relatively simple process without the necessity to involve mechanical or chemical separation methods (Keshk 2014). Moreover, when compared to other types of cellulose, BC presents a higher porosity, higher water retention capacity, higher mechanical strength in its wet state and lower density, as well as a lower production cost (Vasconcelos et al. 2017). Bacterial cellulose is also easy to functionalize, and it can act as a platform for the *in situ* formation of metal and metal oxide nanoparticles, such as silver nanoparticles (Foresti et al. 2017; Valencia et al. 2020), with promising results when tested as an antiseptic for wound-healing applications (Anwar et al. 2022; Barud et al. 2011; Pal et al. 2017).

Silver nanoparticles (AgNPs) are widely-used antiseptics for wound-healing due to their outstanding antibacterial activity (Bruna et al. 2021; Kędziora et al. 2018). Their antimicrobial mechanism deactivates the cell's respiratory enzymes, interrupting the release of adenosine triphosphate and triggering the production of reactive oxygen species, causing a significant damage to both Gram-negative and Gram-positive bacteria (Ahmad et al. 2020; Kalwar and Shan 2018; Ong and Nyam 2022). It is demonstrated that silver nanoparticles can inhibit the growth of *Escherichia coli* (Logambal et al. 2023; Osorio-Echavarría et al. 2022) and *Staphylococcus aureus* (Arokiyaraj et al. 2017; Hasnain et al. 2019), and cellulose–silver composites have been reported to have a remarkable antibacterial activity in multiple studies (Audtarat et al. 2022; Gupta et al. 2020; Homwan et al. 2023; Horue et al. 2020).

For this study, cellulose–silver film composites were synthesized using BC obtained from mothers of vinegar and AgNPs in concentrations of 5, 25, 41, 69, 116 and 324 ppm. Mothers of vinegar are thick and hard layers formed on the surface of vinegar as a product of the acetic fermentation reaction carried out by bacteria of the *Acetobacter* genera (Aykin et al. 2015). The bacteria convert the glucose and glycerol present in the vinegar in a highly pure cellulose with fibrils that are tightly merged into ribbons (Lahiri et al. 2021), which results ideal for immobilizing metal nanoparticles, as well as microorganism cells. The aim of this research was to evaluate BC-AgNPs films as potential topical antiseptics with wound-healing purposes while using BC obtained from mothers of vinegar as a carrier material, as mother of vinegar has been rarely used as a BC source for this purpose despite them being sustainable, affordable, easy to produce and almost entirely composed of cellulose. AgNPs were synthesized through an *in situ* TEMPO-oxidation reaction on BC layers obtained from apple vinegar (avBC) and cranberry vinegar (cvBC). The antibacterial activity and growth inhibition of the films against *Escherichia coli* ATCC-25922 and *Staphylococcus aureus* ATCC-29213 were evaluated.

Experimental

Materials

Chemicals

The reagents used for the TEMPO-mediated oxidation reaction were the following:

2,2,6,6-tetramethylpiperidine-1-oxyl (TEMPO) $C_9H_{18}NO$ (98%) and sodium bromide NaBr (99%) purchased from Sigma-Aldrich, sodium hypochlorite NaOCl (6–9%) from Analytyka, sodium hydroxide NaOH (99%) from Emsure and silver nitrate $AgNO_3$ (99%) from Fermont. Additionally, zinc oxide ZnO (99%) acquired from Sigma-Aldrich was used to perform the cellulose solubility test.

Mother of vinegar

The BC was obtained from mothers of vinegar of two varieties: apple vinegar (avBC) and cranberry vinegar (cvBC). The mothers of vinegar were washed with NaOH 2 M to remove impurities and secondary fermentation products, then washed in distilled water until its pH became neutral. The obtained samples were subjected to a solubility test in a solution of NaOH/ZnO (8:1) at 5 °C, under magnetic stirring to verify that the material obtained was indeed cellulose (Budtova and Navard 2016; Väisänen et al. 2021).

Methods

Samples preparation

The silver nanoparticles were deposited on the BC layers by TEMPO-mediated oxidation, following the method reported by Ifuku et al. (2009) but using wet bacterial cellulose instead of dried cellulose layers and with an *in situ* method variation. The wet BC was chopped and distributed in molds with 5 g per sample. Solutions were prepared with the quantities of TEMPO, NaBr and $AgNO_3$ that were required to synthesize BC-AgNPs films with 5, 25, 41, 69, 116 and 324 ppm, respectively; the quantities were adjusted to obtain films of 0.1 g with areas of approximately 2.5 × 2.5 cm after drying, considering that wet BC layers had 99.5% of water in weight. In all cases, the pH of the solution was maintained between 10.5 and 11 by adding 0.01 M NaOH at room temperature. The solutions were mixed with each sample in their respective molds, and then, the NaOCl solution was added to start the oxidation reaction. Once the reaction finished, the samples were lightly washed with distilled water to remove secondary products and let them to dry in their molds for 2–3 weeks at room temperature.

Sample characterization

The samples were characterized via optical microscopy, Fourier transform infrared spectroscopy (FTIR), thermogravimetric analysis (TGA) and scanning electronic microscopy (SEM). Optical micrographs were obtained with a ZEISS microscope model AX10 (from Oberkochen, Baden-Württemberg, Germany) and visualized with the Motic Images Plus 3.0 software. FTIR analysis was performed in a Perkin-Elmer Spectrophotometer model Spectrum 100 (from Waltham, MA, USA) in the 4000–450 cm^{-1} range, using the KBr plates technique with 200 mg of KBr and 2-mg sample and with a resolution of 4 cm^{-1}. TGA was carried out with a TA Thermogravimetric Analyzer model SDT Q600 (from New Castle, DE, USA) in the 0–600 °C range, with a heating rate of 10 °C min^{-1} and under an N_2 atmosphere. Finally, the SEM micrographs were obtained with a Jeol equipment model JSM IT200 (from Akishima, Tokyo, Japan) using a sample size of approximately 20 mm^2.

Evaluation of antibacterial activity

The antibacterial activity of the BC-AgNPs films against *Escherichia coli* ATCC-25922 and *Staphylococcus aureus* ATCC-29213 was evaluated according to the Japan Industrial Standard JIS Z 2801:2000 (Japanese Standards Association 2000) with minor modifications. The microorganisms were individually grown in trypticase soy broth (TSB) at 37 °C for 24 h. From the obtained culture, a suspension was prepared in 0.85% NaCl solution. The inoculum concentration, calculated through the viable plate count method, was adjusted to approximately 51,000 colony-forming units per milliliter (CFU mL^{-1}) with trypticase soy broth (1/500). Then, 4 mL of this suspension was inoculated into sterile vials containing the sample films. The samples were incubated at 37 °C for 24 h in a humidified atmosphere (90%). After incubation, the resulting suspension was serially diluted, and the number of CFUs was determined by plate counting on trypticase soy agar (TSA) after 24-h incubation at 37 °C. The antibacterial activity (R) was calculated using the next equation:

$$R = \mathrm{Log}\frac{\mathrm{Control}_{24h}}{\mathrm{Control}_{0h}} - \mathrm{Log}\frac{\mathrm{Sample}_{24h}}{\mathrm{Control}_{0h}} \quad (1)$$

where $control_{24h}$ and $control_{0h}$ are the mean number of colonies on the vial without sample film at 24 and 0 h, respectively, while $sample_{24h}$ is the mean number of bacteria on the sample film at 24 h. Finally, the growth inhibition percentage was calculated as follows:

$$\mathrm{Inhibition}(\%) = \frac{\mathrm{CFU}_{\mathrm{control}} - \mathrm{CFU}_{\mathrm{sample}}}{\mathrm{CFU}_{\mathrm{control}}} \times 100 \quad (2)$$

where $CFU_{control}$ and CFU_{sample} are the numbers of colonies at the vial without film and with the film sample, respectively. All tests were conducted in triplicate, and the average values were reported.

Results and discussion

After washing the mothers of vinegar in NaOH, transparent whitish bacterial cellulose layers were obtained. These layers were successfully dissolved in the NaOH/ZnO solution, meaning that they were indeed cellulose, with a degree of polymerization (DP) equal to or less than 200 according to Budtova and Navard (2016) and Väisänen et al. (2021). During the TEMPO-mediated oxidation reaction, the samples changed their color going from yellow to brownish, and finally to grayish, as expected according to Abdellatif et al. (2021). Finally, Fig. 1 shows that the saturation of the colors increased proportionally to the AgNPs concentration, as also reported by Pal et al. (2017).

Characterization of samples

Optical microscopy

Samples of pure bacterial cellulose from both vinegar varieties, as well as cellulose films loaded with 116 ppm of silver nanoparticles, were observed with an optical microscope with 40 × and 75° prism opening, using the polarized mode in order to detect the silver metallic particles. The resulting micrographs are shown in Fig. 2. Although it is not possible to determine the width of the individual cellulose nanofibers with a 40 × magnification, intertwined fibers and strands of about 10–17 µm wide in the case of avBC (a) and about 5–13 µm for the cvBC (b) are visible, as it was expected according to Lahiri et al. (2021). The micrographs of the silver-loaded samples, on the other hand, show that the nanoparticles aggregated and formed blocks as long as 373 and 395 µm in the avBC-AgNPs films (c) and 279 µm in the cvBC-AgNPs films (d). Aggregation likely occurred because of the large specific area of the nanoparticles, which is reported to increase their thermodynamic attraction to each other (Hotze et al. 2010; Tsuda and Konduru 2016).

Fourier transform infrared spectroscopy (FTIR)

Figure 3 shows the FTIR spectra of pure avBC (a) and cvBC (b), as well as the spectra of avBC-AgNPs films (c) and cvBC-AgNPs films (d) with 116 ppm of silver nanoparticles. In all the samples, an O–H stretching can be appreciated at 3340 cm^{-1} and C-H stretchings at 2895, 1424 and 1360 cm^{-1} (Mohite and Patil 2016; Sun et al. 2022). The intensity of the band at 1603 cm^{-1} is higher in the samples with silver nanoparticles; this can be attributed to the increment of carboxylate ions after the TEMPO-oxidation reaction (Feng et al. 2014; Fujii et al. 2020). The peaks that can be observed in all the samples at 1336 and 1314 cm^{-1} correspond to C = O vibrations and skeletal C–C and C–O vibrations, respectively (Abu-Nayem et al. 2020; Sun et al. 2004). The band at 1281 cm^{-1}, which can be observed in the samples with silver, is attributed to vibrations of nitrate groups, probably due to $AgNO_3$ remnants, which was employed as a precursor to obtain the AgNPs (Carvalho et al. 2018; Nunes et al. 2020). The signal at 1250 cm^{-1}, present in the samples with silver nanoparticles, corresponds to an asymmetrical stretching of C–O–C, which also contributes to confirming the carboxyl functionalization of the cellulose (Hong et al. 2021). Observed in all the spectra, the signal at 1206 cm^{-1} represents a C–O stretching band (Nirmala et al. 2011); the peak at 1161 cm^{-1} can be attributed to the C–O–C stretching of the β-glucosidase bonds in the cellulose (Bagewadi et al. 2016; Zhuang et al. 2020); the signal at 1108 cm^{-1} corresponds to the asymmetric C–O–C stretching and C–C breathing mode of cellulose rings (Paladini et al. 2021); the peaks at 1055 and 1032 cm^{-1} are attributed to the C–O–C skeletal vibrations of the pyranose rings in the cellulose (Mohite and Patil 2016; Sun et al. 2004, 2022); the peak at 1004 cm^{-1} corresponds to C–O and C–O–C stretching vibrations in cellulose (Azadfar and Wolcott 2020; Capraru et al. 2022) and the signal at 663 cm^{-1} represents a C–OH out-of-plane bending (Lanzagorta-Garcia et al. 2022). The broad absorption band between 685 and 520 cm^{-1} may be attributed to various vibrations of the pyranose ring and the

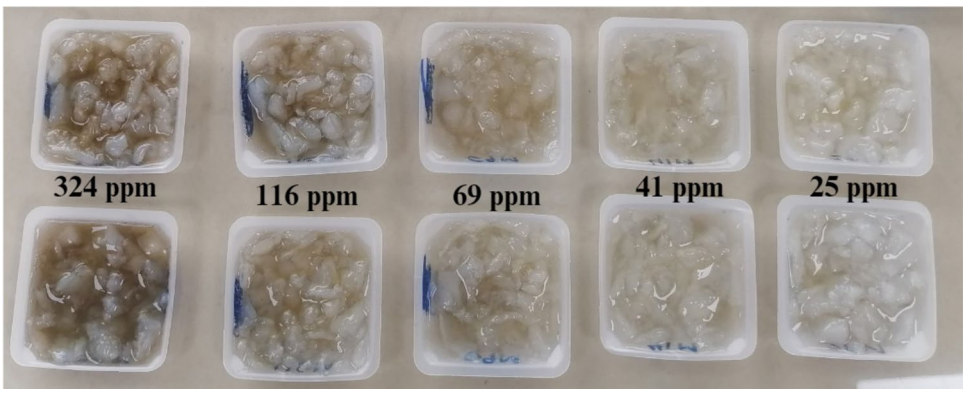

Fig. 1 Samples of avBC loaded with 324, 116, 69, 41 and 25 ppm of silver nanoparticles

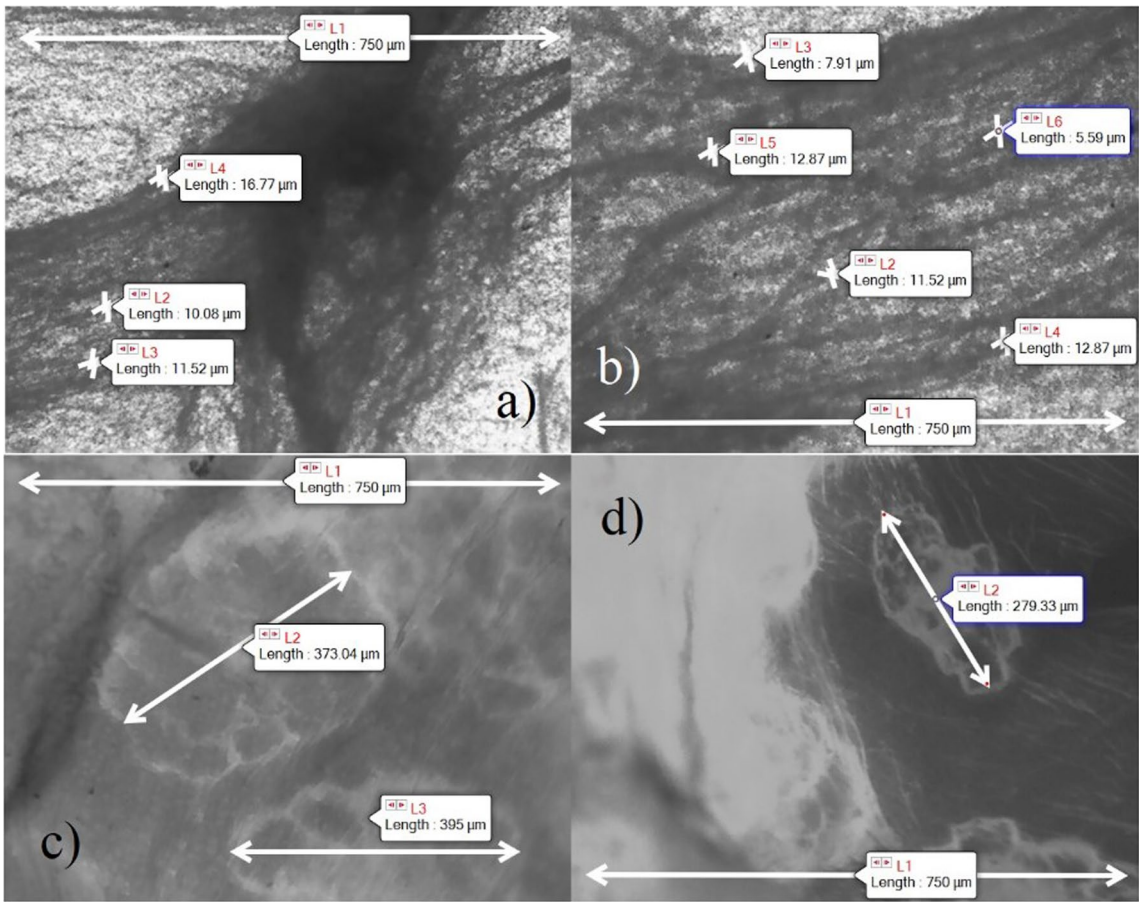

Fig. 2 Optical micrographs of pure avBC **a**, pure cvBC **b**, avBC-AgNPs films **c** and cvBC-AgNPs films **d**

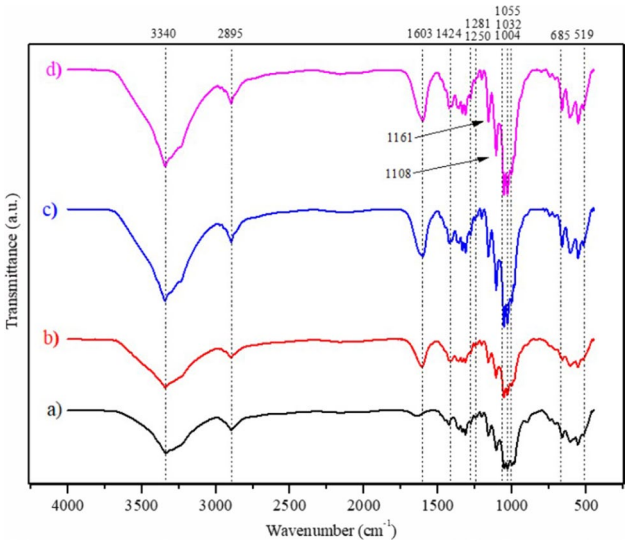

Fig. 3 FTIR spectra of pure avBC **a**, pure cvBC **b**, avBC-AgNPs films **c** and cvBC-AgNPs films **d**

bending vibrations of the hydroxyl groups; and the peak at 519 cm^{-1}, present only in the samples with silver nanoparticles, is attributed to its Ag_2-O stretching vibrations (Alosmanov et al. 2022; Kokot et al. 2002). It is also important to note the absence of signals at 1700 cm^{-1}, indicating that the samples do not contain the carbonyl groups that are characteristic of lignin, which is a confirmation that the cellulose samples are of bacterial and not vegetal origin (Bock et al. 2020; Salim et al. 2021).

Thermogravimetric analysis (TGA)

Thermogravimetric analyses were carried out in the range of 0–600 °C. Figure 4 shows the TGA curves of pure cvBC (a) and cvBC-AgNPs with 116 ppm of silver (b). The first stage of mass loss in the pure BC occurred when heated from room temperature up to 100 °C which corresponds to the loss of moisture in the sample (Mohammadkazemi, et al. 2015; Mutiara et al. 2022). After the water loss, the TGA curve remained stable up to 250 °C, until a slight second degradation stage is observed between 250 and 300 °C, corresponding to the start of the organic compound

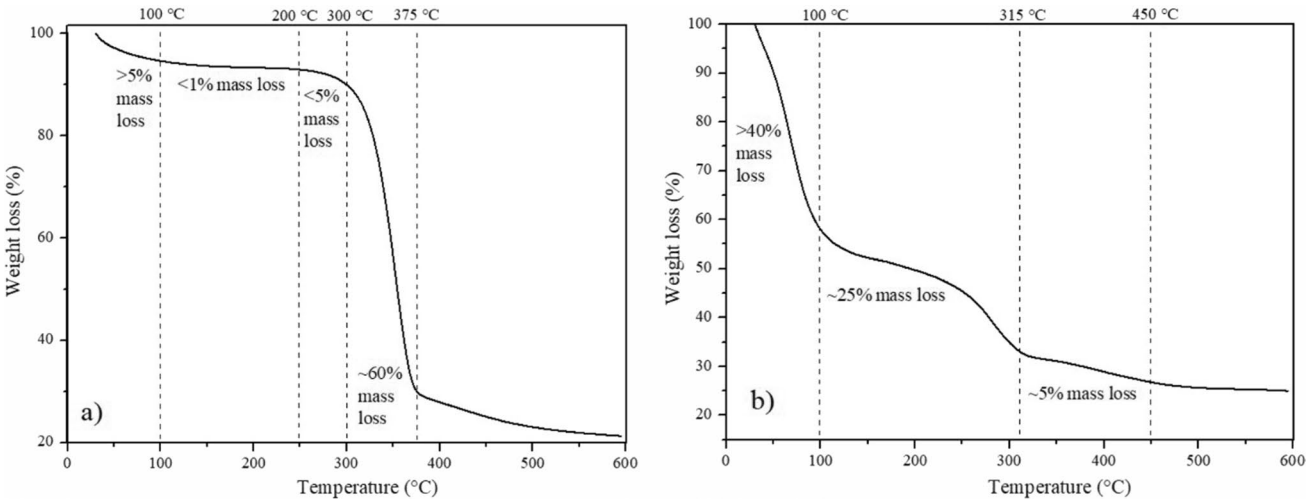

Fig. 4 TGA curves of pure cvBC **a** and cvBC-AgNPs film **b**

decomposition. The third stage in the degradation process, observed from 300 to 375 °C, resulted in a significant weight loss (~60%) and is attributed to the degradation of the cellulose (Mohammadkazemi, et al. 2015; Mutiara et al. 2022). Then, from 375 to 600 °C, there is a fourth and last stage in the degradation process that represents the loss of carbonaceous residues (Zibetti-Teixeira et al. 2019), and the remaining weight corresponds to ashes (Mutiara et al. 2022). Compared to the pure BC samples, the films with silver nanoparticles presented a relatively higher mass loss (> 40%) in the first stage, from room temperature to 100 °C. This is probably due to the degradation of impurities and residues of the synthesis reaction added to the water loss (Labulo et al. 2022). The second degradation stage, from 100 to 315 °C, can be attributed to the loss of the cellulose and organic impurities (Majeed-Khan et al. 2011). The remaining carbonaceous residues decompose during a third degradation stage from 315 to 450 °C (Zibetti-Teixeira et al. 2019). Finally, the TGA curve stabilizes after 500 °C, as the remaining weight corresponds to ashes and the silver nanoparticles (Sampaio and Viana 2018).

The DTG curve observed in Fig. 5a shows that the degradation of the pure cvBC samples occurred in the region of 300–380 °C, with a maximum decomposition rate reached at 353 °C, which is close to the results obtained by Surma-Ślusarska et al. (2008) and Vasil'kov et al. (2023). The DSC curve shown in Fig. 5b corresponds to a cvBC-AgNPs film with 116 ppm of silver, and it presents an intense exothermic peak at 273 °C which can be attributed to the thermal

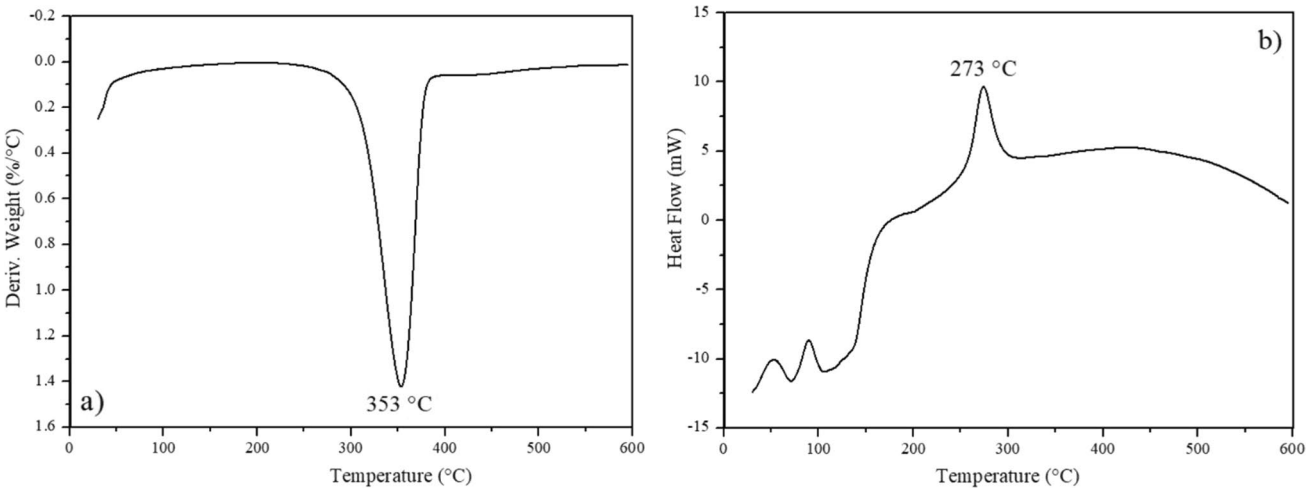

Fig. 5 DTG curve of pure cvBC **a** and DSC curve of cvBC-AgNPs film **b**

decomposition of the cellulose, as expected according to Kristanto et al. (2021) and Majeed-Khan et al. (2011).

Scanning electronic microscopy (SEM)

Figure 6 shows the SEM micrographs of a cvBC-AgNPs film with 116 ppm of silver nanoparticles. It can be observed that most of the silver particles have an average size of 40–50 nm and form clusters with sizes up to 1000 nm (1 µm), as expected according to Chien et al. (2021), de Santa María et al. (2009), Lu et al. (2019) and Mohite and Patil (2016). The Ag/AgCl has not defined shape on the surface of the bacterial nanocellulose.

Antibacterial activity evaluation

Table 1 shows the values of antibacterial activity (R) against *E. coli* and *S. aureus*, as well as the percentage of growth inhibition obtained with the BC-AgNPs films and the pure bacterial cellulose samples. As observed, all the samples with silver nanoparticles presented a high antibacterial activity with R values between 3.37 and 7.72, and according to Nuñez-Figueredo et al. (2019), a material can be considered an effective antibacterial when reaching values of $R \geq 2.0$. Growth inhibition percentages between 99 and 100% confirm that BC-AgNPs films with as low as 5 ppm of silver nanoparticles have potential as antiseptic materials against both bacteria. It is important to mention that the antibacterial activity of all the BC-AgNPs films was higher when tested against *S. aureus* than when tested against *E. coli*. The BC-AgNPs films reached a 100% of growth inhibition with R values between 7.45 and 7.72 and a 99–100% inhibition with R values of 3.37–7.45 against *S. aureus* and *E. coli*, respectively. This finding is in line with the reports of Kawakami et al. (2008), whose research demonstrated that the same metallic element could have different antibacterial properties against different bacteria. It can also be noted that the pure bacterial cellulose samples from both sources showed a slight antibacterial activity against *E. coli*, although not against *S. aureus*. This likely occurred because cellulose fibers have the capacity to immobilize bacteria (Drachuk et al. 2017; Lahiri et al. 2021; Rezaee et al. 2008; Santaolalla et al. 2021). However, this antimicrobial activity is minimal, with R values between 0.04 and 0.13 for *E. coli* and between − 2.84 and − 2.74 for *S. aureus*, with no bacterial growth inhibition in any case.

Finally, it is important to mention that the BC-AgNPs films synthesized for this research equaled or surpassed the values of antibacterial activity and growth inhibition reported for other polymer–silver composites. Polylactide films with 1.0% of silver in weight presented a R value of 4 against *Salmonella enterica* (Martínez-Abad et al. 2013); polysulfone films with 0.2% of a nanohybrid blend of graphene oxide and silver nanoparticles were reported to inhibit the growth of *E. coli* and *S. aureus* in a 83.9% and 58.5%, respectively (Bouchareb et al. 2021); polyethylene films containing Ag-SiO_2 and Ag-TiO_2 mixtures in quantities ranging from 5 to 15% reached growth inhibition values of 99.99% for *S. aureus* and between 92 and 99.97% for *E. coli* (Becaro et al. 2015) and cellulose–AgNPs composites synthesized with plant-extracted cellulose and silver nanoparticles in concentrations of 250 and 500 mM reached values of 99.99% of growth inhibition against *E. coli* (Kwon et al. 2021). Thus, the values of antibacterial activity and growth inhibition reported in this paper show that the bacterial cellulose obtained from mothers of vinegar is a promising material to be used as support for silver nanoparticles with antiseptic purposes, and that the BC-AgNPs composites synthesized with this BC have an effectiveness which is similar to that of the cellulose–silver films produced with cellulose extracted from plants and superior to that of other polymer–silver composites.

Conclusions

In this study, BC-AgNPs films for wound-healing antiseptic purposes were synthesized via TEMPO-mediated oxidation, using mother of vinegar as the source of bacterial cellulose and various silver concentrations within the 5–324 ppm range. The BC was obtained from the mothers of vinegar

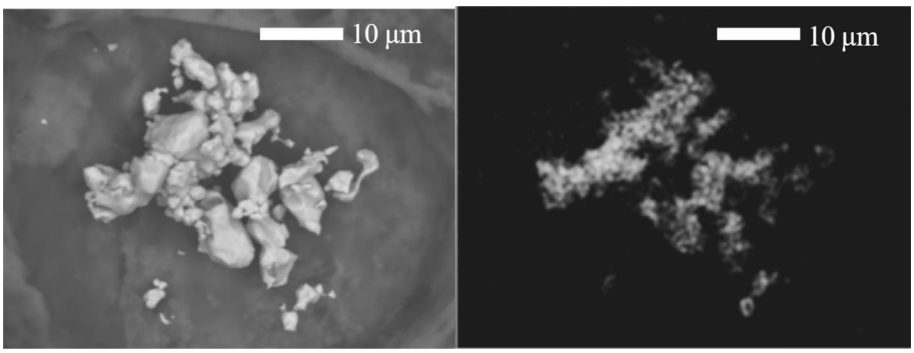

Fig. 6 SEM micrographs of cvBC-AgNPs films

Table 1 Values of antibacterial activity (*R*) and growth inhibition (%) for the BC and BC-AgNPs films against *E. coli* and *S. aureus*

Bacteria	Bacterial cellulose source	Silver nanoparticles concentration (ppm)	Value of antibacterial activity (*R*)	Growth inhibition (%)
Escherichia coli ATCC-25922	Mother of vinegar (apple) avBC	0	0.13	–
		5	5.92	99.90
		25	3.69	99.85
		41	3.49	99.76
		69	3.42	99.72
		116	3.63	99.83
		324	3.55	99.79
	Mother of vinegar (cranberry) cvBC	0	0.04	–
		5	7.45	100
		25	3.61	99.83
		41	3.76	99.87
		69	3.71	99.85
		116	3.37	99.69
		324	3.68	99.84
Staphylococcus aureus ATCC-29213	Mother of vinegar (apple) avBC	0	−2.84	–
		5	7.45	100
		25	7.72	100
		41	7.72	100
		69	7.72	100
		116	7.72	100
		324	7.72	100
	Mother of vinegar (cranberry) cvBC	0	−2.74	–
		5	7.45	100
		25	7.45	100
		41	7.45	100
		69	7.45	100
		116	7.45	100
		324	7.45	100

from two varieties: apple and cranberry. The incorporation of the AgNPs into the bacterial cellulose was verified by optical microscopy, FTIR, TGA and SEM. FTIR and TGA analysis confirmed that the material obtained from the mothers of vinegar was indeed bacterial cellulose. Optical and SEM micrographs revealed that the silver nanoparticles tended to form aggregations, and for this reason, it is recommended to add a stabilizing agent in the future related research. The antimicrobial properties of the BC-AgNPs films were tested against *Staphylococcus aureus* and *Escherichia coli*. The films presented outstanding values of antibacterial effectiveness and achieved a growth inhibition of 99–100% for both bacteria with silver concentrations as low as 5 ppm. These results prove that the BC obtained from mothers of vinegar can be used as an effective carrier for silver nanoparticles with wound-healing purposes, and that the BC-AgNPs composites which were synthesized for this research have great potential as antiseptic materials in the treatment of superficial wounds.

Acknowledgements Abigail M. Díaz-Guerrero acknowledges that she was supported by a postdoctoral fellowship from Consejo Nacional de Humanidades, Ciencias y Tecnologías (CONAHCYT). The authors would like to thank the Tecnológico Nacional de México for the support received through the call for Projects of Scientific Research, Technological Development and Innovation 2024. This research was developed at Tecnológico Nacional de México/Instituto Tecnológico de Ciudad Madero, and the antibacterial activity tests were performed at the Departamento de Materiales Avanzados from Centro de Investigación en Química Aplicada. The authors also appreciate the assistance in grammar and style recommendations by Dr. Omar Alejandro Cabrero Martínez.

Funding The funding was provided by Consejo Nacional de Humanidades, Ciencias y Tecnologías (CONAHCYT), and Tecnológico Nacional de México through the call for Projects of Scientific Research, Technological Development and Innovation 2024 for the project *Antiséptico tópico a base de nanocelulosa bacteriana/nanopartículas de plata: Preparación y caracterización*.

Declarations

Conflict of interest On behalf of all authors, the corresponding author states that there is no conflict of interest.

References

Abdellatif AAH, Alturki H, Tawfeek HM (2021) Different cellulosic polymers for synthesizing silver nanoparticles with antioxidant and antibacterial activities. Sci Rep 11:84. https://doi.org/10.1038/s41598-020-79834-6

Abu-Nayem SM, Sultana N, Aminul-Haque Md, Miah B, Mahmodul Hasan Md, Islam T, Mahedi-Hasan Md, Awal A, Uddin J, Abdul-Aziz Md, Saleh-Ahammad AJ (2020) Green synthesis of gold and silver nanoparticles by using *Amorphophallus paeoniifolius* tuber extract and evaluation of their antibacterial activity. Molecules 25(20):4773. https://doi.org/10.3390/molecules25204773

Ahmad SA, Das SS, Khatoon A, Ansari MT, Afzal M, Hasnain MdS, Nayak AK (2020) Bactericidal activity of silver nanoparticles: a mechanistic review. Mater Sci Technol 3:756–769. https://doi.org/10.1016/j.mset.2020.09.002

Alosmanov R, Buniyat-Zadeh I, Soylak M, Shukurov A, Aliyeva S, Turp S, Guliyeva G (2022) Design, structural characteristic and antibacterial performance of silver-containing cotton fiber nanocomposite. Bioengineering 9:770. https://doi.org/10.3390/bioengineering9120770

Anwar Y, Ul-Islam M, Ali HSHM, Ullah I, Khalil A, Kamal T (2022) Silver impregnated bacterial cellulose-chitosan composite hydrogels for antibacterial and catalytic applications. J Mater Res Technol 18:2037–2047. https://doi.org/10.1016/j.jmrt.2022.03.089

Arokiyaraj S, Vincent S, Saravanan M, Lee Y, Koh Y, Kim KH (2017) Green synthesis of silver nanoparticles using Rheum palmatum root extract and their antibacterial activity against *Staphylococcus aureus* and *Pseudomonas aeruginosa*. Artif Cells Nanomed Biotechnol 45:372–379. https://doi.org/10.3109/21691401.2016.1160403

Audtarat S, Hongsachart P, Dasri T, Chio-Srichan S, Soontaranon S, Wongsinlatam W, Sompech S (2022) Green synthesis of silver nanoparticles loaded into bacterial cellulose for antimicrobial application. Nanocomposites 8(1):34–46. https://doi.org/10.1080/20550324.2022.2055375

Aykın E, Budak NH, Güzel-Seydim ZB (2015) Bioactive components of mother vinegar. J Am Coll Nutr 34(1):80–89. https://doi.org/10.1080/07315724.2014.896230

Azadfar M, Wolcott MP (2020) Surface characterization of powdered cellulose activated by potassium hydroxide in dry condition through ball milling. Polysaccharides 1:80–89. https://doi.org/10.3390/polysaccharides1010006

Bagewadi ZK, Mulla SI, Ninnekar HZ (2016) Purification and characterization of endo β-1,4-D-glucanase from *Trichoderma harzianum* strain HZN11 and its application in production of bioethanol from sweet sorghum bagasse. 3 Biotech 6:101. https://doi.org/10.1007/s13205-016-0421-y

Bakri MKB, Rahman R, Chowdhury FI (2022) Sources of cellulose. In: Rahman R (ed) Fundamentals and Recent Advances in Nanocomposites Based on Polymers and Nanocellulose. Elsevier, Oxford, https://doi.org/10.1016/B978-0-323-85771-0.00012-9

Barud HS, Regiani T, Marques RFC, Lustri WR, Messaddeq Y, Ribeiro SJL (2011) Antimicrobial bacterial cellulose-silver nanoparticles composite membranes. J Nanomater 2011:721631. https://doi.org/10.1155/2011/721631

Becaro AA, Puti FC, Correa DS, Paris EC, Marconcini JM, Ferreira MD (2015) Polyethylene films containing silver nanoparticles for applications in food packaging: characterization of physico-chemical and anti-microbial properties. J Nanosci Nanotechnol 15(3):2148–2156. https://doi.org/10.1166/jnn.2015.9721

Bock P, Nousiainen P, Elder T, Blaukopf M, Amer H, Zirbs R, Potthast A, Gierlinger N (2020) Infrared and raman spectra of lignin substructures: dibenzodioxocin. J Raman Spectrosc 51:422–431. https://doi.org/10.1002/jrs.5808

Bouchareb S, Doufnoune R, Riahi F, Cherif-Silini H, Belbahri L (2021) High performance of polysulfone/graphene oxide-silver nanocomposites with excellent antibacterial capability for medical applications. Mater Today Commun 27:102297. https://doi.org/10.1016/j.mtcomm.2021.102297

Bruna T, Maldonado-Bravo F, Jara P, Caro N (2021) Silver nanoparticles and their antibacterial applications. Int J Mol Sci 22(13):7202. https://doi.org/10.3390/ijms22137202

Budtova T, Navard P (2016) Cellulose in NaOH–water based solvents: a review. Cellulose 23:5–55. https://doi.org/10.1007/s10570-015-0779-8

Capraru O-A, Lungu B, Virgolici M, Constantin M, Cutrubinis M, Chirila L, Cinteza LO, Stanculescu I (2022) Gamma irradiation and Ag and ZnO nanoparticles combined treatment of cotton textile materials. Materials 15:2734. https://doi.org/10.3390/ma15082734

Carvalho I, Ferdov S, Mansilla C, Marques SM, Cerqueira MA, Pastrana LM, Henriques M, Gaidau C, Ferreira P, Carvalho S (2018) Development of antimicrobial leather modified with Ag–TiO_2 nanoparticles for footwear industry. Sci Technol Mater 30(1):60–68. https://doi.org/10.1016/j.stmat.2018.09.002

Chien H-W, Tsai M-Y, Kuo C-J, Lin C-L (2021) Well-dispersed silver nanoparticles on cellulose filter paper for bacterial removal. Nanomaterials 11(3):595. https://doi.org/10.3390/nano11030595

Ciolacu DE, Nicu R, Ciolacu F (2020) Cellulose-based hydrogels as sustained drug-delivery systems. Materials 13(22):5270. https://doi.org/10.3390/ma13225270

Das S, Ghosh B, Sarkar K (2022) Nanocellulose as sustainable biomaterials for drug delivery. S I 3:100135. https://doi.org/10.1016/j.sintl.2021.100135

de Santa Maria LC, Santos ALC, Oliveira PC, Barud HS, Messaddeq Y, Ribeiro SJL (2009) Synthesis and characterization of silver nanoparticles impregnated into bacterial cellulose. Mater Lett 63(9–10):797–799. https://doi.org/10.1016/j.matlet.2009.01.007

Drachuk I, Harbaugh S, Geryak R, Kaplan DL, Tsukruk VV, Kelley-Loughnane N (2017) Immobilization of recombinant *E. coli* cells in a bacterial cellulose-silk composite matrix to preserve biological function. ACS Biomater Sci Eng 3(10):2278–2292. https://doi.org/10.1021/acsbiomaterials.7b00367

Feng J, Shi Q, Li W, Shu W, Chen A, Xie X, Huang X (2014) Antimicrobial activity of silver nanoparticles in situ growth on TEMPO-mediated oxidized bacterial cellulose. Cellulose 21:1557. https://doi.org/10.1007/s10570-014-0449-2

Foresti ML, Vázquez A, Boury B (2017) Applications of bacterial cellulose as precursor of carbon and composites with metal oxide, metal sulfide and metal nanoparticles: A review of recent advances. Carbohydr Polym 157:447–467. https://doi.org/10.1016/j.carbpol.2016.09.008

Fujii Y, Imagawa K, Omura T, Suzuki T, Minami H (2020) Preparation of cellulose/silver composite particles having a recyclable catalytic property. ACS Omega 5(4):1919–1926. https://doi.org/10.1021/acsomega.9b03634

Gupta A, Briffa SM, Swingler S, Gibson H, Kannappan V, Adamus G, Kowalczuk M, Martin C, Radecka I (2020) Synthesis of silver nanoparticles using curcumin-cyclodextrins loaded into bacterial cellulose-based hydrogels for wound dressing

applications. Biomacromol 21(5):1802–1811. https://doi.org/10.1021/acs.biomac.9b01724
Hasnain MS, Javed MdN, Sabir-Alam MdS, Rishishwar P, Rishishwar S, Ali S, Nayak AK, Beg S (2019) Purple heart plant leaves extract-mediated silver nanoparticle synthesis: optimization by Box-Behnken design. Mater Sci Eng C 99:1105–1114. https://doi.org/10.1016/j.msec.2019.02.061
Homwan W, Chaisen K, Audtarat S, Suwonnachot W, Dasri T (2023) Preparation and antibacterial property of silver nanoparticles loaded into bacterial cellulose. Mater Res Express 10:055004. https://doi.org/10.1088/2053-1591/acd991
Hong T, Yin J-Y, Nie S-P, Xie M-Y (2021) Applications of infrared spectroscopy in polysaccharide structural analysis: progress, challenge and perspective. Food Chem: X 12:100168. https://doi.org/10.1016/j.fochx.2021.100168
Horue M, Cacicedo ML, Fernandez MA, Rodenak-Kladniew B, Torres-Sánchez RM, Castro GR (2020) Antimicrobial activities of bacterial cellulose–Silver montmorillonite nanocomposites for wound healing. Mater Sci Eng C 116:111152. https://doi.org/10.1016/j.msec.2020.111152
Hotze EM, Phenrat T, Lowry GV (2010) Nanoparticle aggregation: challenges to understanding transport and reactivity in the environment. J Environ Qual 39(6):1909–1924. https://doi.org/10.2134/jeq2009.0462
Ifuku S, Tsuji M, Morimoto M, Saimoto H, Yano H (2009) Synthesis of silver nanoparticles templated by TEMPO-mediated oxidized bacterial cellulose nanofibers. Biomacromol 10(9):2714–2717. https://doi.org/10.1021/bm9006979
Japanese Standards Association (2000) JIS Z 2801:2000 Antimicrobial Products—Test for Antimicrobial Activity and Efficacy. Japanese Standards Association: Tokyo, Japan.
Kalwar K, Shan D (2018) Antimicrobial effect of silver nanoparticles (AgNPs) and their mechanism–a mini review. Micro Nano Lett 13:277–280. https://doi.org/10.1049/mnl.2017.0648
Kawakami H, Yoshida K, Nishida Y, Kikuchi Y, Sato Y (2008) Antibacterial properties of metallic elements for alloying evaluated with application of JIS Z 2801:2000. ISIJ Int 48(9):1299–1304. https://doi.org/10.23557/isijinternational.48.1299
Kędziora A, Speruda M, Krzyżewska E, Rybka J, Łukowiak A, Bugla-Płoskońska G (2018) Similarities and differences between silver ions and silver in nanoforms as antibacterial agents. Int J Mol Sci 19(2):444. https://doi.org/10.3390/ijms19020444
Keshk J (2014) Bacterial cellulose production and its industrial applications. J Bioproces Biotechniq 4(2):1000150. https://doi.org/10.4172/2155-9821.1000150
Kokot S, Czarnik-Matusewicz B, Ozaki Y (2002) Two-dimensional correlation spectroscopy and principal component analysis studies of temperature-dependent IR spectra of cotton-cellulose. Biopolymers 67(6):456–469. https://doi.org/10.1002/bip.10163
Kristanto J, Azis MM, Purwono S (2021) Multi-distribution activation energy model on slow pyrolysis of cellulose and lignin in TGA/DSC. Heliyon 7:e07669. https://doi.org/10.1016/j.heliyon.2021.e07669
Kwon S, Lee W, Choi JW, Bumbudsanpharoke N, Ko S (2021) A facile green fabrication and characterization of cellulose-silver nanoparticle composite sheets for an antimicrobial food packaging. Front Nutr 8:778310. https://doi.org/10.3389/fnut.2021.778310
Labulo AH, David OA, Terna AD (2022) Green synthesis and characterization of silver nanoparticles using Morinda lucida leaf extract and evaluation of its antioxidant and antimicrobial activity. Chem Pap 76:7313–7325. https://doi.org/10.1007/s11696-022-02392-w
Lahiri D, Nag M, Dutta B, Dey A, Sarkar T, Pati S, Edinur HA, Abdul Kari Z, Mohd Noor NH, Ray RR (2021) Bacterial cellulose: production, characterization, and application as antimicrobial agent. Int J Mol Sci 22(23):12984. https://doi.org/10.3390/ijms222312984
Lanzagorta-Garcia E, Mojicevic M, Milivojevic D, Aleksic I, Vojnovic S, Stevanovic M, Murray J, Adly-Attallah O, Devine D, Brennan-Fournet M (2022) Enhanced antimicrobial activity of biocompatible bacterial cellulose films via dual synergistic action of curcumin and triangular silver nanoplates. Int J Mol Sci 23(20):12198. https://doi.org/10.3390/ijms232012198
Logambal S, Thilagavathi T, Chandrasekar M, Inmozhi C, Ebanda-Kedi PB, Bassyouni FA, Uthrakumar R, Muthukumaran A, Naveenkumar S, Kaviyarasu K (2023) Synthesis and antimicrobial activity of silver nanoparticles: Incorporated couroupita guianensis flower petal extract for biomedical applications. J King Saud Univ Sci 35(1):102455. https://doi.org/10.1016/j.jksus.2022.102455
Lu Y, Luo Y, Lin Z, Huang J (2019) A silver-nanoparticle/cellulose-nanofiber composite as a highly effective substrate for surface-enhanced Raman spectroscopy. Beilstein J Nanotechnol 10:1270–1279. https://doi.org/10.3762/bjnano.10.126
Lukova P, Katsarov P, Pilicheva B (2023) Application of starch, cellulose, and their derivatives in the development of microparticle drug-delivery systems. Polymers 15(17):3615. https://doi.org/10.3390/polym15173615
Majeed-Khan MA, Kumar S, Ahamed M, Alrokayan SA, AlSalhi MS (2011) Structural and thermal studies of silver nanoparticles and electrical transport study of their thin films. Nanoscale Res Lett 6:434. https://doi.org/10.1186/1556-276X-6-434
Martínez-Abad A, Ocio MJ, Lagarón JM, Sánchez G (2013) Evaluation of silver-infused polylactide films for inactivation of Salmonella and feline calicivirus in vitro and on fresh-cut vegetables. Int J Food Microbiol 162(1):89–94. https://doi.org/10.1016/j.ijfoodmicro.2012.12.024
Mohammadkazemi F, Azin M, Ashori A (2015) Production of bacterial cellulose using different carbon sources and culture media. Carbohydr Polym 117:518–523. https://doi.org/10.1016/j.carbpol.2014.10.008
Mohite BV, Patil SV (2016) In situ development of nanosilver-impregnated bacterial cellulose for sustainable released antimicrobial wound dressing. J Appl Biomater Funct Mater 14(1):53–58. https://doi.org/10.5301/jabfm.5000257
Mutiara T, Sulistyo H, Fahrurrozi M, Hidayat M (2022) Facile route of synthesis of silver nanoparticles templated bacterial cellulose, characterization, and its antibacterial application. Green Process Synth 11(1):361–372. https://doi.org/10.1515/gps-2022-0038
Nirmala R, Il BW, Navamathavan R, El-Newehy MH, Kim HY (2011) Preparation and characterizations of anisotropic chitosan nanofibers via electrospinning. Macromol Res 19:345–350. https://doi.org/10.1007/s13233-011-0402-2
Norrrahim MNF, Nurazzi NM, Jenol MA, Farid MAA, Janudin N, Ujang FA, Yasim-Anuar TAT, Najmuddin SUFS, Ilyasf RA (2021) Emerging development of nanocellulose as an antimicrobial material: an overview. Mater Adv 2:3538–3551. https://doi.org/10.1039/D1MA00116G
Nunes S, Ramacciotti F, Neves A, Angelin EM, Ramos AM, Roldão É, Wallaszkovits N, Armijo AA, Melo MJ (2020) A diagnostic tool for assessing the conservation condition of cellulose nitrate and acetate in heritage collections: quantifying the degree of substitution by infrared spectroscopy. Herit Sci 8:33. https://doi.org/10.1186/s40494-020-00373-4
Nuñez-Figueredo Y, Sánchez-Valdes S, Ramírez-Vargas E, Ramos-deValle LF, Albite-Ortega J, Rodriguez-Fernandez OS, Valera-Zaragoza M, Ledezma-Pérez AS, Rodríguez-González AA, Morales-Cepeda AB, Lozano T (2019) Influence of ionic liquid on graphite/silver nanoparticles dispersion and antibacterial properties against *Escherichia coli* of PP/EPDM composite coatings.

J Appl Polym Sci 137(21):48714–48714. https://doi.org/10.1002/APP.48714
Ong WTJ, Nyam KL (2022) Evaluation of silver nanoparticles in cosmeceutical and potential biosafety complications. Saudi J Biol Sci 29(4):2085–2094. https://doi.org/10.1016/j.sjbs.2022.01.035
Osorio Echavarría J, Gómez Vanegas NA, Orozco CPO (2022) Chitosan/carboxymethyl cellulose wound dressings supplemented with biologically synthesized silver nanoparticles from the ligninolytic fungus Anamorphous Bjerkandera sp. R1. Heliyon 8:e10258. https://doi.org/10.1016/j.heliyon.2022.e10258
Pal S, Nisi R, Stoppa M, Licciulli A (2017) Silver-functionalized bacterial cellulose as antibacterial membrane for wound-healing applications. ACS Omega 2(7):3632–3639. https://doi.org/10.1021/acsomega.7b00442
Paladini G, Venuti V, Crupi V, Majolino D, Fiorati A, Punta C (2021) 2D correlation spectroscopy (2DCoS) analysis of temperature-dependent FTIR-ATR spectra in branched polyethyleneimine/TEMPO-oxidized cellulose nano-fiber xerogels. Polymers 13(4):528. https://doi.org/10.3390/polym13040528
Radotić K, Mićić M (2016) Methods for Extraction and Purification of Lignin and Cellulose from Plant Tissues. In: Micic M (ed) Sample Preparation Techniques for Soil Plant and Animal Samples, Springer New York, USA, https://doi.org/10.1007/978-1-4939-3185-9_26
Rezaee A, Godini H, Bakhtou H (2008) Microbial cellulose as support material for the immobilization of denitrifying bacteria. Environ Eng Manag J 7(5):589–594. https://doi.org/10.30638/eemj.2008.082
Salama A, Abouzeid RE, Owda ME, Cruz-Maya I, Guarino V (2021) Cellulose-silver composites materials: preparation and applications. Biomolecules 11:1684. https://doi.org/10.3390/biom11111684
Salim RMd, Asik J, Sarjadi MS (2021) Chemical functional groups of extractives, cellulose and lignin extracted from native *Leucaena leucocephala* bark. Wood Sci Technol 55:295–313. https://doi.org/10.1007/s00226-020-01258-2
Sampaio S, Viana JC (2018) Production of silver nanoparticles by green synthesis using artichoke (*Cynara scolymus* L.) aqueous extract and measurement of their electrical conductivity. Adv Nat Sci: Nanosci Nanotechnol 9(4):045002. https://doi.org/10.1088/2043-6254/aae987
Santaolalla A, Gutierrez J, Gallastegui G, Barona A, Rojo N (2021) Immobilization of *Acidithiobacillus ferrooxidans* in bacterial cellulose for a more sustainable bioleaching process. J Environ Chem Eng 9:105283. https://doi.org/10.1016/j.jece.2021.105283
Sun JX, Sun XF, Zhao H, Sun RC (2004) Isolation and characterization of cellulose from sugarcane bagasse. Polym Degrad Stab 84(2):331–339. https://doi.org/10.1016/j.polymdegradstab.2004.02.008
Sun Z, Li X, Tang Z, Li X, Morrell JJ, Beaugrand J, Yao Y, Zheng Q (2022) Antibacterial films made of bacterial cellulose. Polymers 14(16):3306. https://doi.org/10.3390/polym14163306
Surma-Ślusarska B, Presler S, Danielewicz D (2008) Characteristics of bacterial cellulose obtained from acetobacter xylinum culture for application in papermaking. Fibres Text East Eur 16(4):108–111
Tsuda A, Konduru NV (2016) The role of natural processes and surface energy of inhaled engineered nanoparticles on aggregation and corona formation. NanoImpact 2:38–44. https://doi.org/10.1016/j.impact.2016.06.002
Väisänen S, Ajdary R, Altgen M, Nieminen K, Kesari KK, Ruokolainen J, Rojas OJ, Vuorinen T (2021) Cellulose dissolution in aqueous NaOH–ZnO: cellulose reactivity and the role of ZnO. Cellulose 28:1267–1281. https://doi.org/10.1007/s10570-020-03621-9
Valencia L, Kumar S, Nomena EM, Salazar-Alvarez G, Mathew AP (2020) In-situ growth of metal oxide nanoparticles on cellulose nanofibrils for dye removal and antimicrobial applications. ACS Appl Nano Mater 3(7):7172–7181. https://doi.org/10.1021/acsanm.0c01511
Vasconcelos NF, Andrade-Feitosa JP, Portela da Gama FM, Saraiva Morais JP, Andrade FK, de Souza M, Filho MdS, de Freitas RM (2017) Bacterial cellulose nanocrystals produced under different hydrolysis conditions: properties and morphological features. Carbohydr Polym 155:425–431. https://doi.org/10.1016/j.carbpol.2016.08.090
Vasil'kov A, Butenko I, Naumkin A, Voronova A, Golub A, Buzin M, Sadykova V (2023) Hybrid silver-containing materials based on various forms of bacterial cellulose: synthesis, structure, and biological activity. Int J Mol Sci 24(8):7667. https://doi.org/10.3390/ijms24087667
Wang J, Tavakoli J, Tang Y (2019) Bacterial cellulose production, properties and applications with different culture methods–A review. Carbohydr Polym 219:63–76. https://doi.org/10.1016/j.carbpol.2019.05.008
Zhuang J, Li M, Pu Y, Ragauskas AJ, Yoo CG (2020) Observation of potential contaminants in processed biomass using fourier transform infrared spectroscopy. Appl Sci 10(12):4345. https://doi.org/10.3390/app10124345

Authors and Affiliations

Ana B. Morales-Cepeda[1] · Abigail M. Díaz-Guerrero[1] · Antonio S. Ledezma-Pérez[2] · Carmen N. Alvarado-Canché[2] · José L. Rivera-Armenta[1]

✉ Abigail M. Díaz-Guerrero
abigail.dg@cdmadero.tecnm.mx

[1] Centro de Investigación en Petroquímica, Tecnológico Nacional de México/Instituto Tecnológico de Ciudad Madero, Parque Industrial Tecnia, Bahía de Aldahir S/N, 89603 Altamira, Tamaulipas, Mexico

[2] Departamento de Materiales Avanzados, Centro de Investigación en Química Aplicada, Blvd. Enrique Reyna H. 140, San José de los Cerritos, 25294 Saltillo, Coahuila, Mexico